Are active soft particles suitable for particle jamming actuators?

Chen, Q.; Schott, D.L.; Jovanova, J.

DOI
10.1109/RoboSoft55895.2023.10121929

Publication date
2023

Document Version
Final published version

Published in
Proceedings of the IEEE International Conference on Soft Robotics, RoboSoft 2023

Are active soft particles suitable for particle jamming actuators?

Qianyi Chen[a]*, Dingena Schott[a] , Jovana Jovanova[a]

Abstract — **Soft grippers show adaptability and flexibility in grasping irregularly shaped and fragile objects. However, the soft grippers' low loading capacity and limited shaped fitting ability are the main limitations for developing large-scale applications, especially for heavy objects and objects with sharp edges. The particle jamming effect has emerged as an essential actuation method to adjust the stiffness of soft grippers and enhance the lifting force applied to heavy objects. However, in many large and more serious practical grasping applications, soft actuators are expected to show large scales and several-fold stiffness change, which is challenging to achieve the jamming effect in pneumatic or hydraulic systems. In this paper, a novel active particle jamming method is proposed for the design of a particle jamming-based soft gripper. The proposed method uses active hydrogel particles instead of vacuum pressure to achieve the jamming effect. Additionally, the bending behaviors are implemented based on the jamming effect and actuator design. The numerical model is carried out to explore the actuator behaviors, and a brief experiment case is conducted to verify the feasibility. The results indicated that the proposed actuator achieves the functionality of bending actions by swelling the hydrogel particles. The bending performance is enhanced by lowering the trigging temperature and increasing the thickness of the strain-limit layer. Additionally, there is a transition state from bending to curling when increasing the layer of particles.**

Keywords: **Soft gripper, Particle jamming, Hydrogel, Actuator, Numerical simulation**

I. INTRODUCTION

It is always a big challenge to grasp complex objects in robotics. Robotic grippers, which contact objects directly, must interact with the environment or human beings to perform various tasks in different application scenarios [1]. Traditional robotic grippers are designed based on low rigid controllers that attach to complex sensors and predefined kinematics systems, which always perform poorly in grasping irregularly shaped, flexible, or fragile objects [2, 3].

Due to their flexible body, soft grippers have better mechanical properties and interaction capabilities than traditional rigid grippers [4, 5]. Hence, soft grippers can grasp delicate objects with safety and an easy control process [6]. Soft grippers can be powered by different kinds of actuators that use different methods, such as electrical or magnetic charge [7, 8], shape memory effect [9], chemical reaction [10], and fluidic pressures [11]. The various actuators can support the soft grippers with low cost and high efficiency.

However, limited to the compliance and the lack of robustness of the soft materials, soft robotic grippers have always been used on objects across a range of scales only from hundreds of μm to a few centimeters and perform poorly with large-scale or heavy objects [12]. Inspiringly, the promising properties of using the jamming effect in stiffness variation bring the possibility of solving this problem [13]. The first particle jamming based gripper was designed by Brown et al. [14], which can grasp various irregular objects without active feedback. Since then, many researchers have been working on new soft robot designs based on the jamming principle.

The principle of particle jamming effects can be described as two states [15]. The particles are loosely packed inside a membrane sac with low stiffness in the initial state. Thus the particles can move quickly. When the air inside the sac is evacuated, atmospheric pressure will be exerted on the particle system, resulting in enhanced interaction forces between particles and the system's stiffness. A particle jamming based soft finger was designed by Wei [16]. A pneumatic actuator drives the bending motion, and the heavier object can be grasped since the particle chamber provides a stiffness-changing interface between the particles and the finger membrane. Although particle jamming has generated much research interest in stiffness variation, most previous robotic designs suffer from bulky vacuum pumps, which limit their portability and usability in large-scale applications [17].

In this study, a novel particle jamming based soft gripper is proposed based on active deformable particles. First, the proposed actuator utilizes active deformable particles, which can achieve large deformation. Furthermore, the experimental cases and simulation results dedicated dynamic system is not required for the actuator. The active particles can expand or deform by environmental triggers. In addition, the behaviors of particles induce the jamming effect, resulting in higher stiffness.

Qianyi Chen is with the Department of Maritime and Transport Technology, Faculty of Mechanical, Maritime and Materials Engineering, Delft University of Technology, Delft, 2628CD, The Netherlands (corresponding author to provide phone: +310613989827; e-mail: Q.Chen-5@tudelft.nl).

Dingena Schott is with the Department of Maritime and Transport Technology, Faculty of Mechanical, Maritime and Materials Engineering, Delft University of Technology, Delft, 2628CD, The Netherlands (e-mail: D.L.Schott@tudelft.nl).

Jovana Jovanova is with the Department of Maritime and Transport Technology, Faculty of Mechanical, Maritime and Materials Engineering, Delft University of Technology, Delft, 2628CD, The Netherlands (e-mail: J.Jovanova@tudelft.nl).

2023 IEEE International Conference on Soft Robotics (RoboSoft) | 979-8-3503-3222-3/23/$31.00 ©2023 IEEE | DOI: 10.1109/ROBOSOFT55895.2023.10121929

II. Jamming Effect with Deformable Particles

A. Mechanism of the active soft particle jamming effect.

Typically, the particle jamming effect achieves by the pneumatic system. Our design uses smart deformable particles instead to accomplish the jamming effect. As shown in Fig. 1, different soft particles fill the chamber, which can achieve the action of expanding or deforming by external stimuli. After the dynamic behaviors, the arrangement of particles and the total volume of the particle group will change. Thus, particles jam with each other due to the increasing interaction between particles.

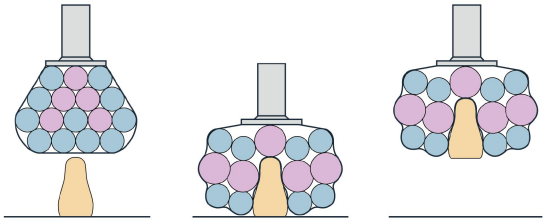

Fig. 1. Illustration of the active particle jamming actuator

Additionally, active soft particles' jamming process differs from rigid particles. As shown in Fig. 2, a critical packing density point occurs when particles start to contact each other. The jamming will form in the crucial packing din the crucial the rigid particles. However, the soft particles are necessary to jump over the point jamming to reach the jamming state. When the packing density is over a critical point, the soft particles will deform by the interaction forces. In this case, the friction forces decrease, and the bulk and shear modulus vanish, resulting in the jamming state. Additionally, at the jamming state, the packing density of soft particles is higher, which means that they can compact more and achieve higher stiffness.

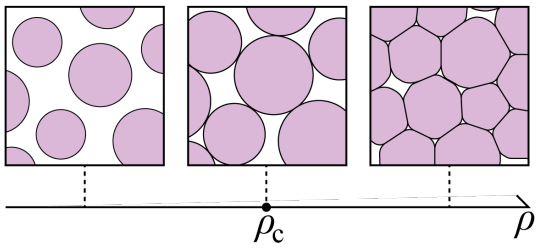

Fig. 2. Packing state of active particle jamming process

B. Design of the active particle jamming actuator

Based on the active jamming effects, the design of the actuator is shown in Fig.3. As shown in Fig.3, the covered membrane is made of conventional elastic material. Moreover, the hydrogel particles fill the chamber. The strain-limit layer sets on the left, the top of the actuator is fixed, and the bottom of the actuator is the free end. In the working state, the hydrogel particles are stimulated by the temperature change. They will jam each other and interact with the membrane, resulting in the expanding trend of the structure. However, However, the strain-limit layer restricts the stretching of the left membrane, causing the overall design to bend toward the left.

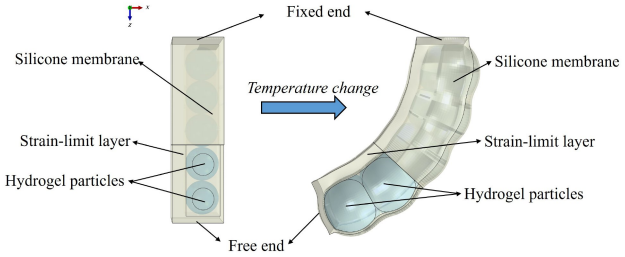

Fig. 3. The working process of the actuator

In addition, the actuator's geometric parameters are defined in Fig. 4. The thickness of the left is t_0, which sets to 2 mm. The thicknesses at the top and bottom are t_1, which is set to 4 mm. In addition, the width of the strain-limit layer, h. Furthermore, the initial hydrogel particles Furthermore, the initial hydrogel particles have a diameter, d, of 16 mm.

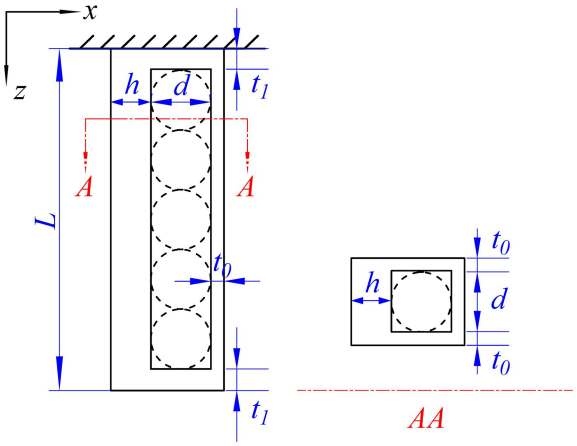

Fig. 4. A front view and the cross-section view of the actuator structure.

Further, to validate the feasibility of the design, the brief experiment case is conducted as proof of the discipline. As shown in Fig. 5, the hydrogel particles fill the chamber. The covered membrane and Strain-limit layer are silicone (Ecoflex-30). Also, the water injects into the cavity as the triggering medium. After the swelling of the hydrogel particles, it can be seen that the overall structure is bent to the left, indicating that the designed actuator can achieve the expected function.

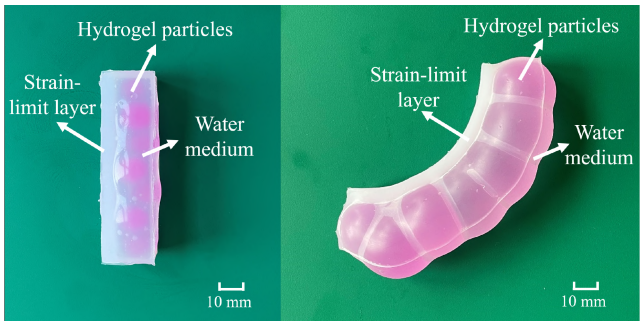

Fig. 5. The demonstration of the active soft particles for particles jamming

III. Methodology

Hydrogel, a water-swollen soft active material, exhibits marked volume change and is widely used in soft robotics [18]. Temperature-sensitive hydrogel poly (PNIPAM) hydrogel, which has attracted intense attention due to its unique features, such as simplicity of synthesis and high stability, is used in our design.

The commercial finite element software ABAQUS, combined with a user-defined subroutine, is used for the PNIPAM hydrogel.

Treating hydrogel as a hyperelastic material and adopting the nonlinear field theory of coupled diffusion and deformation [19], the free energy of the hydrogel describes as,

$$W(I_1, I_3, \mu, T) = \frac{1}{2} N k_B T (I_1 - 3 - 2\log I_3) - \frac{k_B T}{\nu}\left[(I_3 - 1)\log\frac{I_3}{I_3 - 1} + \frac{\chi(T, I_3)}{I_3}\right] - \frac{\mu}{\nu}(I_3 - 1) \quad (1)$$

where $I_1 = F_{iK}F_{iK}$ and $I_3 = \det \mathbf{F}$ are the first and the third invariants of the deformation gradient tensor. Moreover, μ is the chemical potential, T is the temperature, N is the number of chains per polymer volume, ν is the volume of a solvent molecule, and k_B is the Boltzmann constant.

Additionally, the Flory–Huggins interaction parameter, χ, measures the enthalpy of the mixing process and is expressed in terms of T and I_3 for a temperature-sensitive hydrogel,

$$\chi(T, I_3) = A_0 + B_0 T + \frac{A_1 + B_1 T}{I_3} \quad (2)$$

The experiments can take the coefficients Ai and Bi as $A_0 = -12.947$, $B_0 = 0.0449\ \mathrm{K}^{-1}$, $A_1 = 17.92$, $B_1 = -0.0569\ \mathrm{K}^{-1}$ [20]. In addition, the expression of stresses immediately follows, and the first Piola–Kirchhoff stress is computed as,

$$\mathbf{P} = \frac{\partial W_0(I_1, I_3)}{\partial \mathbf{F}} = \frac{\partial W_0(I_1, I_3)}{\partial I_1}\frac{\partial I_1}{\partial \mathbf{F}} + \frac{\partial W_0(I_1, I_3)}{\partial I_3}\frac{\partial I_3}{\partial \mathbf{F}} \quad (3)$$

In the simulations, we normalize the stresses and Young's modulus of materials by $k_B T/\nu$, which is estimated as 4×10^7 Pa. The hydrogel is assumed to be in a homogeneous free-swollen state after synthesis before being integrated into the all-polymer structure. An initial swelling ratio, λ_0, which equals for all three directions, is characterized in this state. Different synthesis conditions yield various initial swelling ratios, and without loss of generality, λ_0 is fixed to 1.5 in the calculation, which corresponds to an equilibrium chemical potential of $\mu = -0.0343$ for the material of the hydrogel [21].

IV. Results and Discussion

In the following simulation cases, influential parameters, including temperature, the number of particle layers, and the thickness of the strain-limit layer, are input as boundary conditions to explore the bending performance. Additionally, the bending performance is evaluated by the bending angle and displacement (δ) at the free end.

A. Effects of the temperature

This section analyzes the effects on the bending angle, and the displacement of different temperatures (T) applied to the hydrogel particles. In addition, the initial particle layer sets to 5, and other geometry parameters are as defined in Fig. 4.

As shown in Fig. 6, the bending state shows a significant difference in the temperature from 275 K to 295 K. In the higher-temperature atmosphere, the hydrogel particles shrink due to the release of water, resulting in less interaction with the membrane and a decrease in the bending angle. On the contrary, the hydrogel particles swell when the temperature is lowered due to water absorption. In this situation, particles undergo large deformation because they jam each other. Also, the actuator bends to the right because of the strain-limit layer.

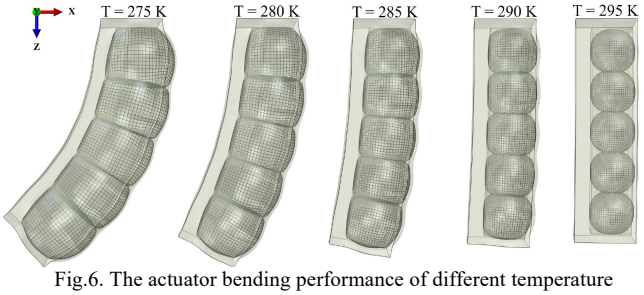

Fig.6. The actuator bending performance of different temperature

Furthermore, the displacements in the horizontal direction (x direction) and vertical direction (z direction) are shown in Fig. 7.

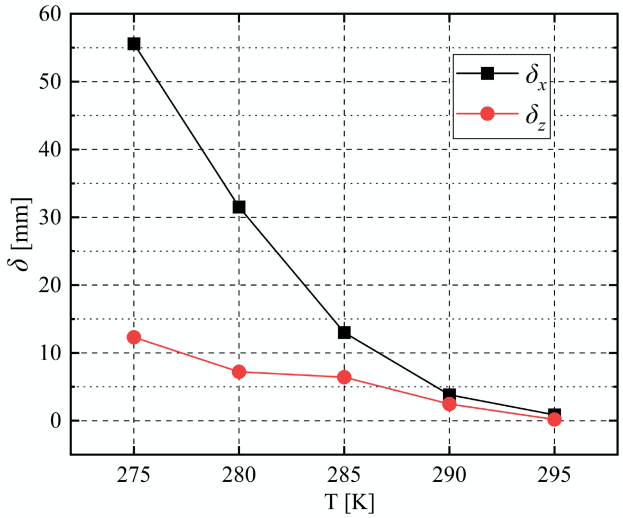

Fig. 7. The displacements of the actuator of different trigged temperatures in different directions

Similarly, the displacements decrease with increasing temperature and show a linear trend. Specifically, as the temperature decreases, the change in the removal in the horizontal direction is more pronounced, which indicates that the pulling action of the strain-limit layer provides more force to help the actuator bend in the jamming state.

B. Effects of the particle layers

This section analyzes the effects on the bending performance and the displacement of different particle layers

(PL) from 5 to 19. The trigger temperature condition sets to 275 K, and other parameters are defined in Fig.4.

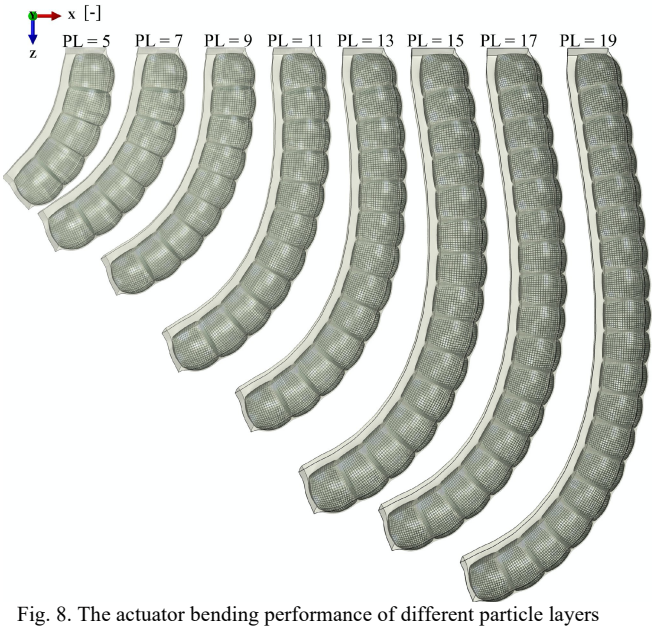

Fig. 8. The actuator bending performance of different particle layers

The bending performances of different particle layers are shown in Fig. 8. First, the particle layers' final bending angle increases from 5 to 9, while the bending angle drops gradually from 9 to 19. In addition, when the particle layer is over 9, the actuator exhibits a specific curvature near the fixed end rather than only at the free end. There is a change in the bending state between the number of particle layers from 9 to 10. This change can explain the transition from a bending state to a curling state. When the number of particle layers is small, the length of the actuator is also at a low level. At this time, the internal force produced by the interactions between hydrogel particles and membrane takes most of the effects on the structure in the horizontal direction. Thus the bending state forms. However, when the number of particle layers increases, the soft design is too long to fully support each particle's independent swelling. Thus the internal force produced by the interactions between particles begins to take effect in the vertical direction, resulting in the curling state.

Additionally, the displacements of different directions at the free end are shown in Fig.9 to explore the detailed actions of the actuator of different particle layers. It can be seen that the displacement in the horizontal direction increases first of the particle layers from 5 to 9 and remains stable from 9 to 19. In addition, the displacement in the vertical direction increases of particle layers from 5 to 7 and then drops down from 7 to 19, which indicates that in the curling state, increasing the number of particle layers does not result in more horizontal displacement at the free. Instead, the vertical displacement decreases slightly. Combined with Fig. 8, increasing the number of particle layers will make the curling state more apparent, and the structure of the actuator tends to be more arc-shaped, which is conducive to grasping or wrapping slender and bulky objects.

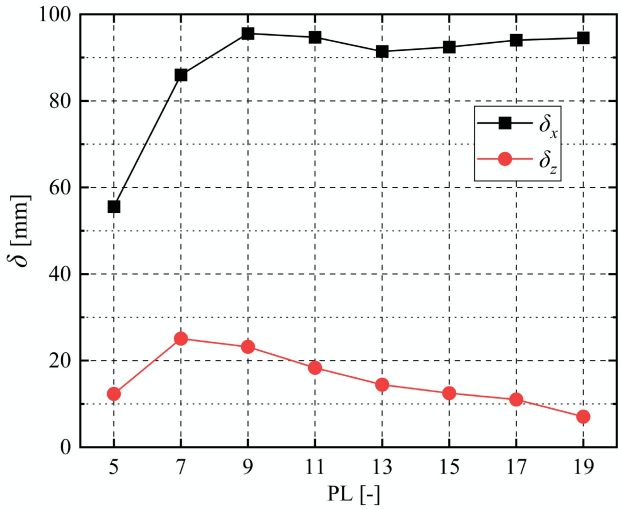

Fig. 9. The displacements of the actuator of different numbers of particle layers in different directions.

C. *Effects of the thickness of the strain-limit layer*

This section analyzes the effects on the bending angle and the displacement of different thicknesses of the strain-limit layer. In addition, the initial particle layer sets to 5, the trigger temperature is set to 275 K, and other geometry parameters are defined in Fig. 4.

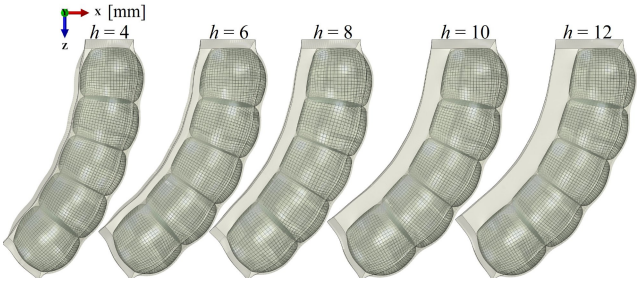

Fig.10. The actuator bending performance of different strain-limit layer

The bending performances of different thicknesses (h) of the strain-limit layer from 4 mm to 12 mm are shown in Fig. 10. Generally, the bending angle increases obviously of the thickness from 4 mm to 12mm. Specifically, the bending rise increases rapidly of the thickness from 4 mm to 10 mm. In contrast, the bending angle remains the thickness from 10 mm to 12 mm, which indicates that the existence of the strain-limit layer has a good effect on the bending performance of the actuator. Also, the bending performance can be improved by adequately increasing the strain-limit layer's thickness.

To explore the complex bending behaviors of different strain-limit layers, the actuator's displacements of different directions at the free end are described in Fig. 11.

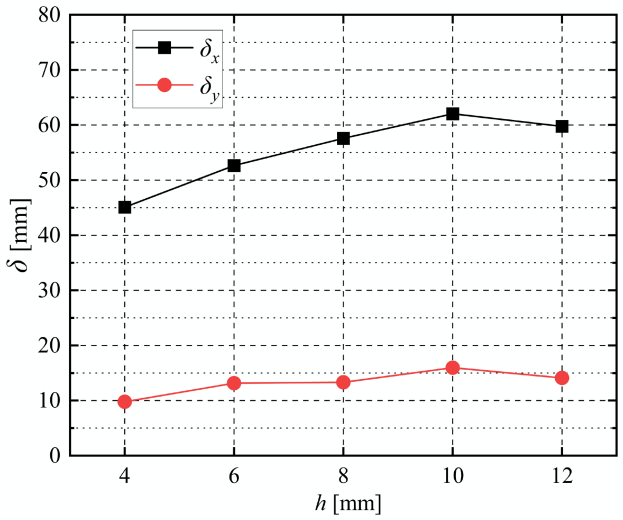

Fig.11. The displacements of different thicknesses of the strain-limit layer in different directions.

First, the displacements in the horizontal and vertical directions increase when the thickness is from 4 mm to 10 mm, indicating that a thicker strain-limit layer helps the actuator obtain more displacements, thereby improving the bending performance. However, the displacements decrease when the thickness is from 10 mm to 12 mm, which indicates that the negative effect produces when the thickness is too thick. A thicker strain-limit layer requires more force to generate strain. Therefore, when the strain-limit layer thickens, the deformation on the left side is limited, helping the overall structure to bend more towards the left. However, when the strain-limit layer is too thick, the tensile effect itself exceeds the interaction caused by the swelling of the hydrogel particles. Thus the internal force is insufficient to deform the structure, resulting in less bending displacements.

V. Conclusion

Current soft actuators based on the particle jamming effect limit the range of applications because of the actuation method. This study proposed a novel active particle jamming based actuator to explore the potential of the application on large scales. The soft actuator based on the hydrogel particles is characterized by a deformable chamber and a strain-limit layer.

The brief experiment case was conducted to validate the effect of the actuator. In addition, the numerical method was developed to quantify the influence of design parameters on the bending performance. Both the experimental case and simulation results illustrated that the proposed design could actively achieve the bending actions trigged by water medium and temperature change. In addition, the specific simulation results showed that better bending performance could be achieved by decreasing the temperature and increasing the number of particle layers from 5 to 9. Also, the bending performance can be enhanced by increasing the thickness of the strain-limit layer. Furthermore, there is a transition from a bending state to a curling state when increasing the number of particle layers over 9.

The proposed actuator will support completing the design, modeling, and fabrication of a soft grasping gripper actuator with actively stimulated particles or membrane. Also, the dual-chamber and triple-chamber structures filled with different active deformable particles will develop to achieve bilateral bending and twisting actions.

VI. Acknowledgment

This work is supported by the National Natural Science Foundation of China Grant No. 52071240, the Higher Education Discipline Innovation Project Grant No. BP0820028, and China Scholarship Council Grant No. 202006950011. The financial contributions are gratefully acknowledged.

.

References

[1] J. Krüger, T. K. Lien, and A. Verl, “Cooperation of human and machines in assembly lines,” *CIRP annals,* vol. 58, no. 2, pp. 628-646, 2009.

[2] A. M. Okamura, N. Smaby, and M. R. Cutkosky, "An overview of dexterous manipulation." pp. 255-262.

[3] N. Xydas, M. Bhagavat, and I. Kao, "Study of soft-finger contact mechanics using finite elements analysis and experiments." pp. 2179-2184.

[4] D. Rus, and M. T. Tolley, “Design, fabrication and control of soft robots,” *Nature,* vol. 521, no. 7553, pp. 467-475, 2015.

[5] K.-J. Cho, J.-S. Koh, S. Kim, W.-S. Chu, Y. Hong, and S.-H. Ahn, “Review of manufacturing processes for soft biomimetic robots,” *International Journal of Precision Engineering and Manufacturing,* vol. 10, no. 3, pp. 171-181, 2009.

[6] E. Coevoet, T. Morales-Bieze, F. Largilliere, Z. Zhang, M. Thieffry, M. Sanz-Lopez, B. Carrez, D. Marchal, O. Goury, and J. Dequidt, “Software toolkit for modeling, simulation, and control of soft robots,” *Advanced Robotics,* vol. 31, no. 22, pp. 1208-1224, 2017.

[7] U. Gupta, L. Qin, Y. Wang, H. Godaba, and J. Zhu, “Soft robots based on dielectric elastomer actuators: a review,” *Smart Materials and Structures,* vol. 28, no. 10, pp. 103002, 2019.

[8] X. Li, Z. Zhang, M. Sun, H. Wu, Y. Zhou, H. Wu, and S. Jiang, “A magneto-active soft gripper with adaptive and controllable motion,” *Smart Materials and Structures,* vol. 30, no. 1, pp. 015024, 2020.

[9] E. Hamburg, V. Vunder, U. Johanson, F. Kaasik, and A. Aabloo, "Soft shape-adaptive gripping device made from artificial muscle." p. 97981Q.

[10] M. Wehner, R. L. Truby, D. J. Fitzgerald, B. Mosadegh, G. M. Whitesides, J. A. Lewis, and R. J. Wood, “An integrated design and fabrication strategy for entirely soft, autonomous robots,” *Nature,* vol. 536, no. 7617, pp. 451-455, 2016.

[11] B. Mosadegh, P. Polygerinos, C. Keplinger, S. Wennstedt, R. F. Shepherd, U. Gupta, J. Shim, K. Bertoldi, C. J. Walsh, and G. M. Whitesides, “Pneumatic networks for soft robotics that actuate rapidly,” *Advanced functional materials,* vol. 24, no. 15, pp. 2163-2170, 2014.

[12] I. D. Walker, D. M. Dawson, T. Flash, F. W. Grasso, R. T. Hanlon, B. Hochner, W. M. Kier, C. C. Pagano, C. D. Rahn, and Q. M. Zhang, "Continuum robot arms inspired by cephalopods." pp. 303-314.

[13] S. G. Fitzgerald, G. W. Delaney, and D. Howard, "A Review of Jamming Actuation in Soft Robotics." p. 104.

[14] E. Brown, N. Rodenberg, J. Amend, A. Mozeika, E. Steltz, M. R. Zakin, H. Lipson, and H. M. Jaeger, “Universal robotic gripper based on the jamming of granular material,” *Proceedings of the National Academy of Sciences,* vol. 107, no. 44, pp. 18809-18814, 2010.

[15] Y. Wei, "Investigations of variable stiffness principles for compliant robotics," *HKU Theses Online (HKUTO)*, 2016.
[16] Y. Wei, Y. Chen, T. Ren, Q. Chen, C. Yan, Y. Yang, and Y. Li, "A novel, variable stiffness robotic gripper based on integrated soft actuating and particle jamming," *Soft Robotics,* vol. 3, no. 3, pp. 134-143, 2016.
[17] Y. Yang, Y. Li, and Y. Chen, "Principles and methods for stiffness modulation in soft robot design and development," *Bio-Design and Manufacturing,* vol. 1, no. 1, pp. 14-25, 2018.
[18] P. Calvert, "Hydrogels for soft machines," *Advanced materials,* vol. 21, no. 7, pp. 743-756, 2009.
[19] W. Hong, Z. Liu, and Z. Suo, "Inhomogeneous swelling of a gel in equilibrium with a solvent and mechanical load," *International Journal of Solids and Structures,* vol. 46, no. 17, pp. 3282-3289, 2009.
[20] S. Cai, and Z. Suo, "Mechanics and chemical thermodynamics of phase transition in temperature-sensitive hydrogels," *Journal of the Mechanics and Physics of Solids,* vol. 59, no. 11, pp. 2259-2278, 2011.
[21] W. Guo, M. Li, and J. Zhou, "Modeling programmable deformation of self-folding all-polymer structures with temperature-sensitive hydrogels," *Smart Materials and Structures,* vol. 22, no. 11, pp. 115028, 2013.